VIP *The following Communications have been judged by at least two referees to be "very important papers" and will be published online at www.angewandte.org soon:*

*F. P. C. Binder, K. Lemme, R. C. Preston, B. Ernst**
Sialyl Lewis^x: A "Pre-organized Water Oligomer"?

R. Liu, G. Yuan, C. L. Joe, T. E. Lightburn, K. L. Tan, D. Wang**
Silicon Nanowires as Photoelectrodes for Carbon Dioxide Fixation

Editorial

"… Major challenges in drug discovery may inspire chemical biology research and by extension, organic synthesis endeavors. Conversely, the outcomes of a chemical biology investigation may fuel efforts in drug discovery …"
Read more in the Editorial by Herbert Waldmann.

H. Waldmann* ———— **6284 – 6285**

Drug Discovery … The Third in the Band!

Author Profile

"Looking back over my career, I would say that some detours were worth it.
When I was eighteen I wanted to be a chemistry student, however, first I had to spend one year in the army …"
This and more about Frank Würthner can be found on page 6308.

Frank Würthner ———— **6308 – 6309**

News

B. List

M. Christmann

K. Müllen

Otto Bayer Award: B. List ———— **6310**

Young Scientist Award for Natural Product Research:
M. Christmann ———— **6310**

BASF Award for Organic Electronics and Einstein Professorship:
K. Müllen ———— **6310**

Books

Supramolecular Photochemistry — V. Ramamurthy, Yoshihisa Inoue — *reviewed by A. Credi* ———— **6311**

Highlights

Bacterial Communication

R. J. Worthington,
C. Melander* ——— 6314–6315

Deconvoluting Interspecies Bacterial Communication

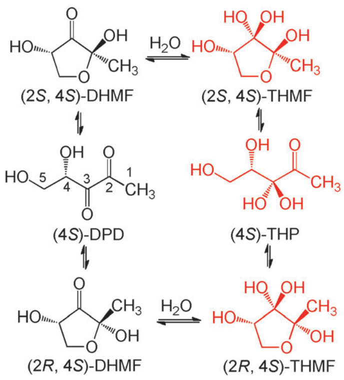

The universal bacterial signal molecule autoinducer-2 (AI-2) is derived from 4,5-dihydroxy-2,3-pentanedione (DPD). DPD exists in a complex equilibrium between multiple forms (see scheme), and NMR spectroscopy has now been used to establish that the extent of the structural diversity displayed by DPD over a broad pH range is even greater than previously posited.

Lewis Acidic Cyclophanes

F. P. Gabbaï* ——— 6316–6318

Incorporation of Boron in the Walls of an "All-Carbon" Cyclophane: A Novel Approach to Lewis Acidic Macrocycles

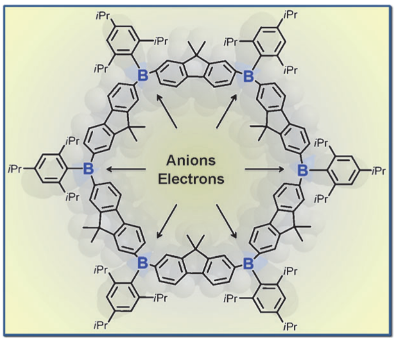

A p-doped conjugated cyclophane! The six boron atoms of the bora-cyclophane (see picture) recently reported by Chen and Jäkle team up to impart a set of unique properties to this novel macrocycle. In particular, this macrocycle undergoes six consecutive reversible reductions to afford the hexaanion. It also binds up to six small nucleophilic anions, a process that quenches the fluorescence of the ring and changes its character to electron-rich.

Minireviews

Molecular Scaffolds

D. M. Beal, L. H. Jones* —— 6320–6326

Molecular Scaffolds Using Multiple Orthogonal Conjugations: Applications in Chemical Biology and Drug Discovery

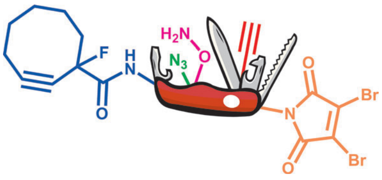

More tools, please! The toolbox of synthetic transformations that facilitate chemistry at the interface with biology, particularly in a pharmaceutical setting, is still far from adequate. Heteromultifunctional scaffolds (represented by the pocket knife in the picture) suitable for sequential "click" reactions have been developed recently that may find significant utility in the areas of chemical biology and chemically enabled biotherapeutics.

For the USA and Canada: ANGEWANDTE CHEMIE International Edition (ISSN 1433-7851) is published weekly by Wiley-VCH, PO Box 191161, 69451 Weinheim, Germany. Air freight and mailing in the USA by Publications Expediting Inc., 200 Meacham Ave., Elmont, NY 11003. Periodicals postage paid at Jamaica, NY 11431. US POSTMASTER: send address changes to *Angewandte Chemie*, Journal Customer Services, John Wiley & Sons Inc., 350 Main St., Malden, MA 02148-5020. Annual subscription price for institutions: US$ 11.738/10.206 (valid for print and electronic / print or electronic delivery); for individuals who are personal members of a national chemical society prices are available on request. Postage and handling charges included. All prices are subject to local VAT/sales tax.

Reviews

Supramolecular Chemistry

D. Görl, X. Zhang,
F. Würthner* ________ 6328 – 6348

Molecular Assemblies of Perylene Bisimide Dyes in Water

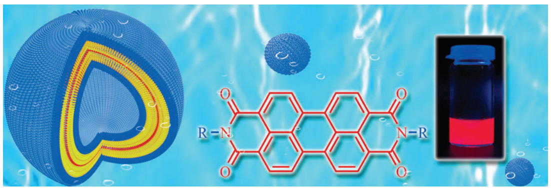

Fascinating functional nanostructures are formed in water by amphiphilic perylene bisimide dyes through strong hydrophobic interactions. This Review describes the current developments in the self-assembly of perylene bisimides in water to form π–π-stacked molecular aggregates.

Communications

Electrochemistry

A. Elahi, T. Fowowe,
D. J. Caruana* ________ 6350 – 6355

Dynamic Electrochemistry in Flame Plasma Electrolyte

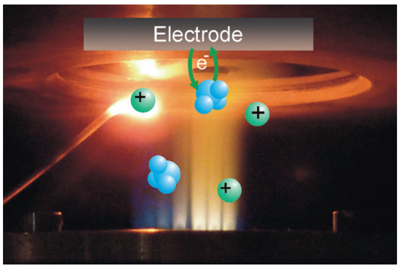

Chemistry in flames: Dynamic electrochemistry in the gas phase is described by considering the ionized medium of a flame as an electrolyte (see picture). This study opens up the possibility of accessing redox reactions that are outside the potential limits set by the solvent in conventional liquid-phase electrochemistry.

Frontispiece

Gaseous Organometallics

G.-L. Hou, H. Wen, K. Lopata, W.-J. Zheng,
K. Kowalski, N. Govind, X.-B. Wang,*
S. S. Xantheas* ________ 6356 – 6360

A Combined Gas-Phase Photoelectron Spectroscopic and Theoretical Study of Zeise's Anion and Its Bromine and Iodine Analogues

Shining light on Zeise: In a study of Zeise's anion, $[PtCl_3(C_2H_4)]^-$, and its bromine and iodine analogues, electronic structure information for each species, derived from spectral features, is assigned through calculations at the coupled cluster level of theory. The calculations indicate that the electron binding energies decrease with halogen size and that there is a synergistic η^2 interaction between C_2H_4 and the PtX_3^- anions.

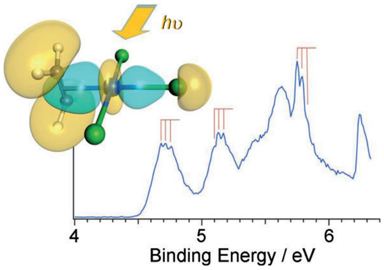

Front Cover

Photoswitchable Magnetism

M. Nihei, Y. Okamoto, Y. Sekine,
N. Hoshino, T. Shiga, I. P.-C. Liu,
H. Oshio* ________ 6361 – 6364

A Light-Induced Phase Exhibiting Slow Magnetic Relaxation in a Cyanide-Bridged $[Fe_4Co_2]$ Complex

Single-molecule magnets: A cyanide-bridged hexanuclear complex showed a thermal electron-transfer-coupled spin transition centered at 220 K. Light irradiation at low temperature (LT; HT = high temperature) generated a metastable state showing slow magnetic relaxation in measurements of the alternating-current magnetic susceptibility (χ_m; see picture).

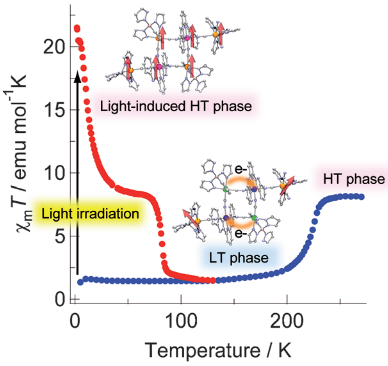

Back Cover

Heteronanostructures

S. K. Han, M. Gong, H. B. Yao,
Z. M. Wang, S. H. Yu* **6365 – 6368**

One-Pot Controlled Synthesis of Hexagonal-Prismatic $Cu_{1.94}S$-ZnS, $Cu_{1.94}S$-ZnS-$Cu_{1.94}S$, and $Cu_{1.94}S$-ZnS-$Cu_{1.94}S$-ZnS-$Cu_{1.94}S$ Heteronanostructures

Inside Back Cover

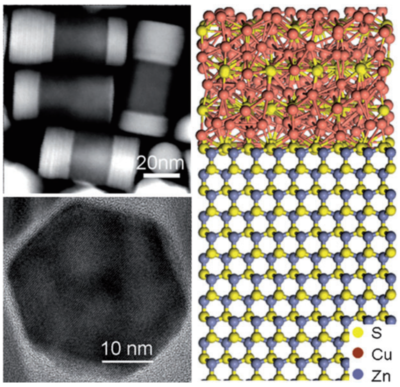

Playing six-a-side: Complex hexagonal prism $Cu_{1.94}S$-ZnS heteronanostructures were synthesized by a colloidal route. $Cu_{1.94}S$-ZnS, $Cu_{1.94}S$-ZnS-$Cu_{1.94}S$, and $Cu_{1.94}S$-ZnS-$Cu_{1.94}S$-ZnS-$Cu_{1.94}S$ structures are formed with screw-, dumbbell-, and sandwich-like shapes by using CuI and $[Zn(S_2CNEt_2)_2]$ as precursors in oleylamine.

RNA Structures

Y. Sato, T. Ichihashi, S. Nishizawa,
N. Teramae* **6369 – 6372**

Strong and Selective Binding of Amiloride to an Abasic Site in RNA Duplexes: Thermodynamic Characterization and MicroRNA Detection

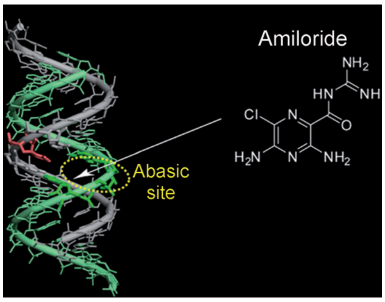

Firmly tied: The binding affinity of amiloride for an abasic (AP) site-containing RNA duplex (see picture) is two orders of magnitude superior to the affinity of the corresponding AP site-containing DNA duplex. The observed high binding affinity for the RNA duplex arises from a favorable enthalpy gain. The binding-induced fluorescence response of amiloride is applicable to microRNA detection.

Self-Assembly

Y. Liu, X. Han, L. He, Y. Yin* **6373 – 6377**

Thermoresponsive Assembly of Charged Gold Nanoparticles and Their Reversible Tuning of Plasmon Coupling

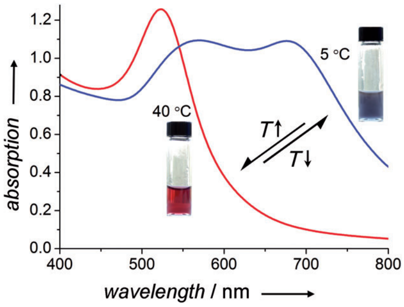

Charged colloidal gold nanoparticles (AuNPs) can be assembled and disassembled in an aqueous solution in response to temperature change and display reversible thermoresponsive tuning of plasmon coupling. The reversible tuning was made possible by manipulating the electrostatic interaction through the temperature-dependent zeta potential of the charged AuNPs (see the extinction spectra of a typical AuNP dispersion).

Nanotubes

S. Sengupta, D. Ebeling, S. Patwardhan,
X. Zhang, H. von Berlepsch, C. Böttcher,
V. Stepanenko, S. Uemura, C. Hentschel,
H. Fuchs, F. C. Grozema,
L. D. A. Siebbeles, A. R. Holzwarth,
L. F. Chi,* F. Würthner* **6378 – 6382**

Biosupramolecular Nanowires from Chlorophyll Dyes with Exceptional Charge-Transport Properties

Conductive tubes: Self-assembled nanotubes of a bacteriochlorophyll derivative are reminiscent of natural chlorosomal light-harvesting assemblies. After deposition on a substrate that consists of a non-conductive silicon oxide surface (see picture, brown) and contacting the chlorin nanowires to a conductive polymer (yellow), they show exceptional charge-transport properties.

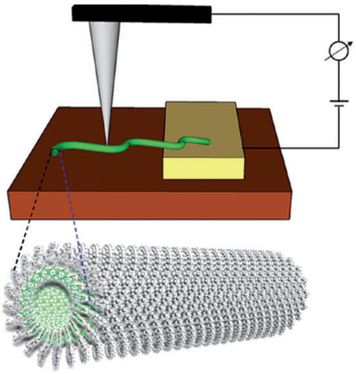

The German Chemical Society (GDCh) invites you to:

Angewandte Anniversary Symposium

125 JAHRE

GDCh

Eine Zeitschrift der Gesellschaft Deutscher Chemiker

Tuesday, March 12, 2013

Henry Ford Building / FU Berlin

Speakers


Carolyn R.
Bertozzi


François
Diederich


Alois
Fürstner


Roald Hoffmann
(Nobel Prize 1981)


Susumu
Kitagawa


Jean-Marie Lehn
(Nobel Prize 1987)


E.W. „Bert“
Meijer


Frank
Schirrmacher
(Publisher, *FAZ*)


Robert
Schlögl


George M.
Whitesides


Ahmed Zewail
(Nobel Prize 1999)

More information:

angewandte.org/symposium

Freie Universität Berlin

WILEY-VCH

GDCh
GESELLSCHAFT
DEUTSCHER CHEMIKER

PSJ_12_42497_5_gu

Photoluminescence

J. E. Park, M. Son, M. Hong, G. Lee, H. C. Choi* ______ **6383 – 6388**

Crystal-Plane-Dependent Photoluminescence of Pentacene 1D Wire and 2D Disk Crystals

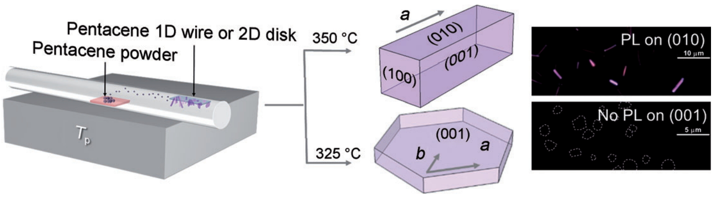

Down to the wire: Pentacene exhibits crystal-plane-dependent photoluminescence (PL) activity, as demonstrated in highly crystalline 1D wires and 2D disks, which were selectively synthesized using the vaporization–condensation–recrystallization (VCR) process. Although pentacene 1D wires and 2D disks have identical triclinic crystal structures, PL activity is observed only from pentacene 1D wires owing to the presence of "PL-active" (010) planes.

Nanotube Toxicology

K. T. Al-Jamal, A. Nunes, L. Methven, H. Ali-Boucetta, S. Li, F. M. Toma, M. A. Herrero, W. T. Al-Jamal, H. M. M. ten Eikelder, J. Foster, S. J. Mather, M. Prato,* A. Bianco,* K. Kostarelos* ______ **6389 – 6393**

Degree of Chemical Functionalization of Carbon Nanotubes Determines Tissue Distribution and Excretion Profile

Getting rid of the tubes: An assessment of the retention of functionalized multi-walled carbon nanotubes (MWNTs) in the organs of mice was carried out using single photon emission computed tomography and quantitative scintigraphy (see scheme). Increasing the degree of functionalization on MWNTs enhanced renal clearance, while lower functionalization promoted reticuloendethelial system accumulation.

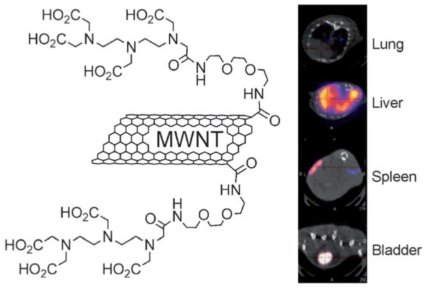

Metal–Metal Multiple Bonds

S.-C. Liu, W.-L. Ke, J.-S. K. Yu,* T.-S. Kuo, Y.-C. Tsai* ______ **6394 – 6397**

An Electron-Rich Molybdenum–Molybdenum Quintuple Bond Spanned by One Lithium Atom

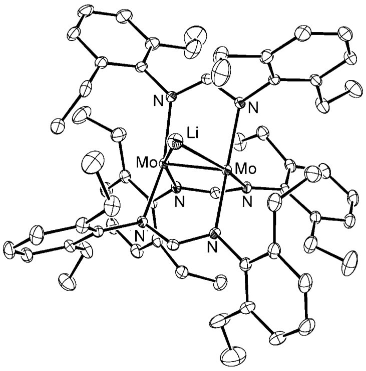

Take five: A unique quintuply bonded dimolybdenum complex $[Mo_2(\mu\text{-Li})\{\mu\text{-HC(N-2,6-Et}_2C_6H_3)_2\}_3]$ (see picture) was synthesized and characterized. The Mo–Mo interaction includes an unexpected bridging Li^+ ion. Calculations indicate the bridging Li^+ ion does not perturb the Mo–Mo bond length (2.0612(4) Å), but results in a relatively small effective Mo–Mo bond order of 3.67.

Mechanochromic Luminescence

M. J. Teng, X. R. Jia,* X. F. Chen, Y. Wei ______ **6398 – 6401**

A Dipeptide-Based Multicolored-Switching Luminescent Solid Material: When Molecular Assemblies Meet Mechanochemical Reaction

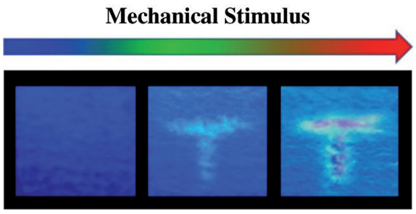

Color schemes: A mechanochromic material composed of two types of peptides bearing a pyrene group and rhodamine B moieties, respectively, displays multiluminescent colors, such as blue, green, and reddish in one sample (see picture). The mechanochromic behavior is based on a combined switching of molecular assemblies and chemical structure.

Cycloaddition

J. D. Kirkham, R. J. Butlin,
J. P. A. Harrity* ____________ **6402 – 6405**

A Mild Benzannulation through Directed Cycloaddition Reactions

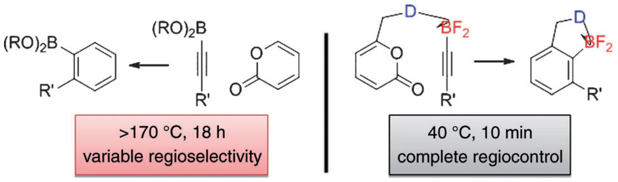

Simple as ABC: Alkynyl borane cycloadditions can be substrate-directed to assemble aromatic difluoroboranes within an extremely mild and efficient reaction manifold compared to that of traditional methods (see scheme). The aromatic boranes are readily transformed into a range of useful products.

Catalytic Microspheres

Z. Jin, M. D. Xiao, Z. H. Bao, P. Wang,
J. F. Wang* ____________ **6406 – 6410**

A General Approach to Mesoporous Metal Oxide Microspheres Loaded with Noble Metal Nanoparticles

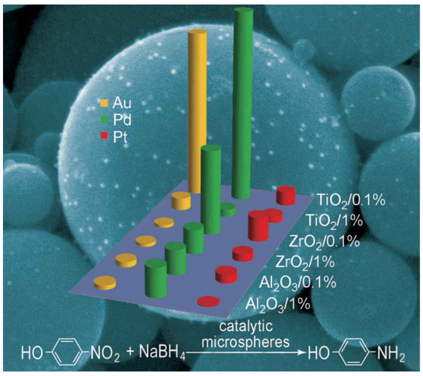

Catalytic microspheres: A general approach is demonstrated for the facile preparation of mesoporous metal oxide microspheres loaded with noble metal nanoparticles (see TEM image in the picture). Among 18 oxide/noble metal catalysts, TiO_2/0.1 mol% Pd microspheres showed the highest turnover frequency in $NaBH_4$ reduction of 4-nitrophenol (see picture).

Biomineralization

C. B. Mao,* F. Wang, B. Cao **6411 – 6415**

Controlling Nanostructures of Mesoporous Silica Fibers by Supramolecular Assembly of Genetically Modifiable Bacteriophages

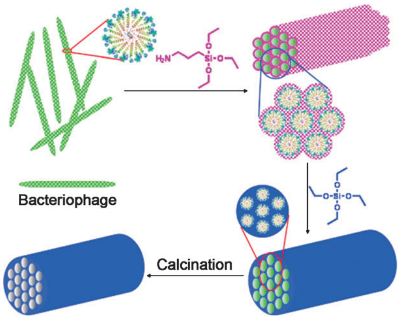

A useful virus: The synthesis of a new family of mesoporous silica fibers is reported. Monodisperse filamentous bacteriophages self-assembled into highly ordered hexagonal lattices that were used as templates for the formation of silica nanostructures. Removal of the bacteriophage assembly through calcination led to the formation of mesoporous silica fibers with pore structures precisely defined by the bacteriophage assembly (see picture).

Artificial Cells

C. Martino, S.-H. Kim, L. Horsfall,
A. Abbaspourrad, S. J. Rosser, J. Cooper,*
D. A. Weitz* ____________ **6416 – 6420**

Protein Expression, Aggregation, and Triggered Release from Polymersomes as Artificial Cell-like Structures

Bringing droplets to life: A cytoskeletal protein (red dots, see scheme) is expressed in artificial cells composed of biocompatible polymersomes, which encapsulate expression machinery and amino acid building blocks. Release of the expressed proteins can be triggered by a negative osmotic shock.

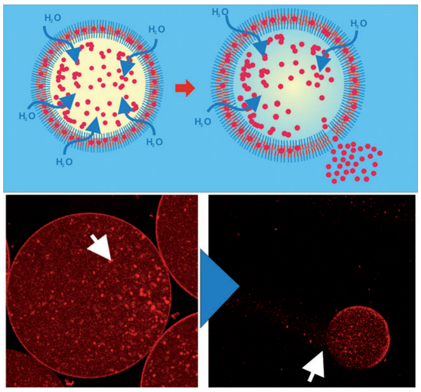

Graphene

M.-E. Ragoussi, J. Malig, G. Katsukis,
B. Butz, E. Spiecker, G. de la Torre,*
T. Torres,* D. M. Guldi* ____ **6421 – 6425**

Linking Photo- and Redoxactive Phthalocyanines Covalently to Graphene

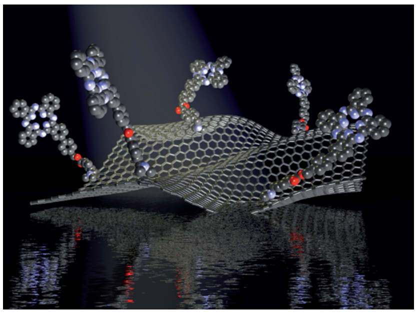

“Green” graphene: For the first time, the covalent attachment of a light-harvesting and electron-donating phthalocyanine to the basal plane of few-layer graphene is reported (see picture). Physicochemical characterizations reveal an ultrafast charge separation from the photoexcited phthalocyanine to few-layer graphene followed by a slower charge recombination.

Supramolecular Systems

S. Cantekin, H. M. M. t. Eikelder,
A. J. Markvoort, M. A. J. Veld,
P. A. Korevaar, M. M. Green,
A. R. A. Palmans,*
E. W. Meijer* ____________ **6426 – 6431**

Consequences of Cooperativity in Racemizing Supramolecular Systems

Saluting the sergeant: Phg-BTA (see scheme) cooperatively self-assembles into helical aggregates and shows unprecedented racemization behavior in the presence of base. In thermodynamically controlled conditions, the addition of a small amount of chiral auxiliary to this mixture results in a deracemization reaction and a final enantiomeric excess of 32%. A theoretical model is presented to understand in detail the results obtained.

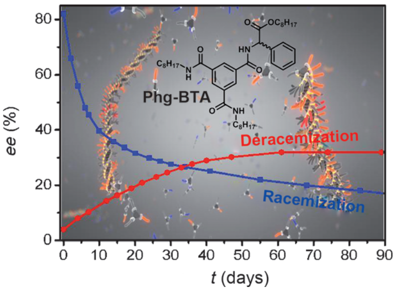

Fluorescent Probes

W. Shi,* X. H. Li, H. M. Ma* **6432 – 6435**

A Tunable Ratiometric pH Sensor Based on Carbon Nanodots for the Quantitative Measurement of the Intracellular pH of Whole Cells

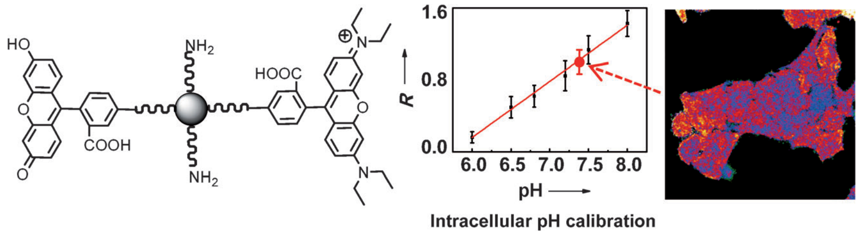

The whole picture: Carbon nanodots labeled with two fluorescent dyes have been developed as a tunable ratiometric pH sensor to measure intracellular pH. The nanosensor shows good biocompatibility and cellular dispersibility. Quantitative determinations on intact HeLa cells and pH fluctuations associated with oxidative stress were performed.

Peptide Conformations

M. Tirado, N. C. Polfer* ____ **6436 – 6438**

Defying Entropy: Forming Large Head-to-Tail Macrocycles in the Gas Phase

Spectral fingerprints: Collision-induced dissociation (CID) of protonated peptides in the gas phase results in linear fragment ions with a five-membered oxazolone ring on their C-terminal side. Infrared spectroscopy confirms that smaller fragments adopt oxazolone structures. Conversely, in mid-sized and larger fragments an isomerization to “head-to-tail” macrocycles is observed (see picture).

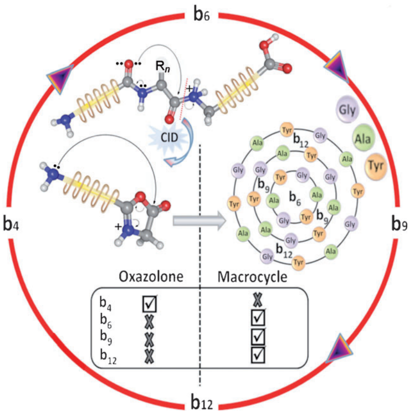

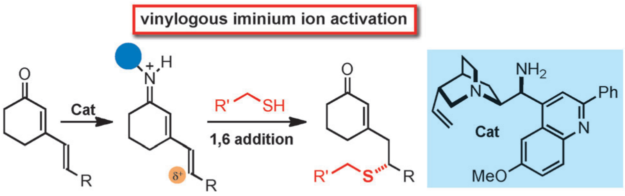

Remote transmission: In the presence of chiral amines, 2,4-dienones are activated toward the attack of a nucleophile at the δ position, a mode of activation that is termed vinylogous iminium ion catalysis. Specifically, the 1,6 addition of alkyl thiols to β-substituted cyclic dienones was catalyzed by a cinchona-based primary amine; the reaction was highly stereoselective and displayed high selectivity for reaction at the δ position.

Asymmetric Organocatalysis

X. Tian, Y. Liu,
P. Melchiorre* ———— **6439 – 6442**

Aminocatalytic Enantioselective 1,6 Additions of Alkyl Thiols to Cyclic Dienones: Vinylogous Iminium Ion Activation

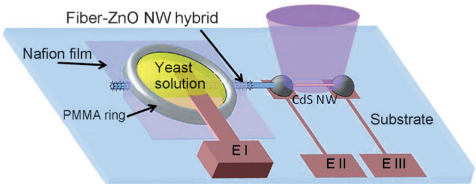

An integrated system consisting of a carbon fiber–ZnO hybrid nanowire (NW) multicolor photodetector is driven by a microbial fuel cell (see picture; PMMA = poly(methyl methacrylate), E = electrode). The self-powered photodetector can detect at light levels of as little as nW cm^{-2} intensity with a responsivity of more than 300 A W^{-1}.

Self-Powered Nanophotonics

Q. Yang, Y. Liu, Z. Li, Z. Yang, X. Wang,
Z. L. Wang* ———— **6443 – 6446**

Self-Powered Ultrasensitive Nanowire Photodetector Driven by a Hybridized Microbial Fuel Cell

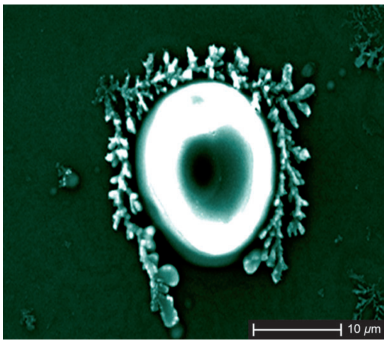

Meet at the border: Assembly of the water-soluble cobalt tetrakis(*N*-methylpyridinium-4-yl)porphyrin [CoTMPyP]$^{4+}$ at soft interfaces is enhanced and stabilized by its interfacial interaction with the lipophilic anion $(C_6F_5)_4B^-$. The supramolecular structure thus formed (see picture) provides excellent catalytic activity in the four-electron reduction of oxygen.

Interfacial Self-Assembly

A. J. Olaya, D. Schaming, P.-F. Brevet,
H. Nagatani, H.-J. Xu, M. Meyer,
H. H. Girault* ———— **6447 – 6451**

Interfacial Self-Assembly of Water-Soluble Cationic Porphyrins for the Reduction of Oxygen to Water

It goes both ways: A thiol-reactive cross-linker based on a bridged azobenzene derivative permits photoreversible control of peptide conformation on irradiation with violet (407 nm) and green (500–550 nm) light (see picture) through isomerization of the cross-linker. The large separation of the absorbance bands of the *cis* (yellow) and *trans* (red) isomers enables complete bidirectional photoswitching.

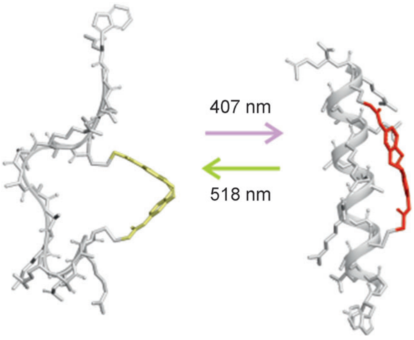

Photoisomerization

S. Samanta, C. Qin, A. J. Lough,
G. A. Woolley* ———— **6452 – 6455**

Bidirectional Photocontrol of Peptide Conformation with a Bridged Azobenzene Derivative

VIP

Biosensors

L. M. H. Lai, I. Y. Goon, K. Chuah, M. Lim, F. Braet, R. Amal, J. J. Gooding* ______ **6456 – 6459**

The Biochemiresistor: An Ultrasensitive Biosensor for Small Organic Molecules

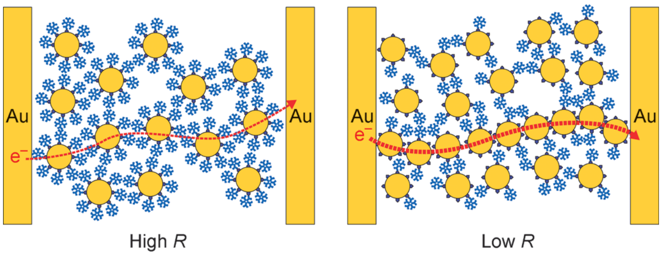

New sensation: A resistance-based biosensor uses gold-coated magnetic nanoparticles (Au@MNPs) functionalized with the antibiotic enrofloxin (see picture; purple), which bind to anti-enrofloxin as analyte (blue). The Au@MNPs can be magnetically assembled between electrodes, and the measured resistance *R* is a function of analyte concentration.

NMR Spectra Without Multiplets

J. A. Aguilar, A. A. Colbourne, J. Cassani, M. Nilsson, G. A. Morris* ______ **6460 – 6463**

Decoupling Two-Dimensional NMR Spectroscopy in Both Dimensions: Pure Shift NOESY and COSY

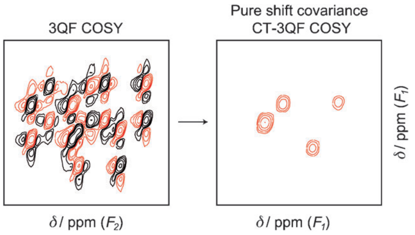

An increase in the resolving power in 2D NMR spectra is obtained by collapsing 2D signals with multiplet structure into 2D singlets. This resolution gain is achieved by combining 2D experiments with pure shift techniques and covariance processing (see picture). The method should be of value in both manual and automated structure determination.

Metal-Containing DNA

T. Funai, Y. Miyazaki, M. Aotani, E. Yamaguchi, O. Nakagawa, S. Wada, H. Torigoe, A. Ono, H. Urata* ______ **6464 – 6466**

Ag^I Ion Mediated Formation of a C–A Mispair by DNA Polymerases

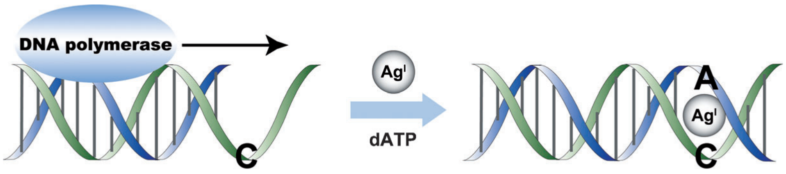

Silver turns up the A–C: In the presence of Ag^I ions, a DNA polymerase incorporated deoxyadenosine (from dATP) at the site opposite cytosine in the template strand to afford the full-length product (see scheme), meaning that DNA polymerases prefer a C-Ag^I-A base pair to the more thermodynamically stable C-Ag^I-C base pair.

Enantiospecific Catalysis

V. Bizet, X. Pannecoucke, J. L. Renaud,* D. Cahard* ______ **6467 – 6470**

Ruthenium-Catalyzed Redox Isomerization of Trifluoromethylated Allylic Alcohols: Mechanistic Evidence for an Enantiospecific Pathway

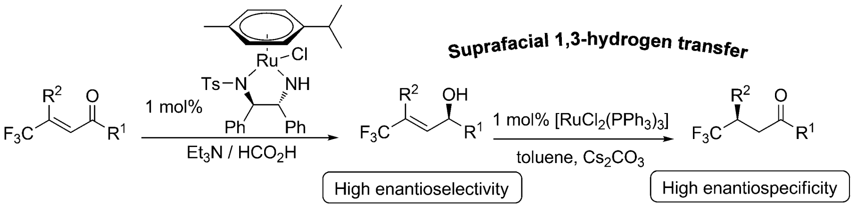

Transfer news: A synthetic approach to chiral β-CF_3-substituted saturated carbonyl compounds has been developed in which ruthenium complexes efficiently catalyze the redox isomerization of CF_3-bearing allylic alcohols by an intramolecular suprafacial enantiospecific 1,3-hydrogen transfer (see scheme). This method was used for the enantioselective synthesis of (*S*)-CF_3-citronellol.

Heterocycles

M. Yamagishi, K. Nishigai, A. Ishii, T. Hata, H. Urabe* ________ **6471 – 6474**

Facile Preparation of Indoles and 1,2-Benzothiazine 1,1-Dioxides: Nucleophilic Addition of Sulfonamides to Bromoacetylenes and Subsequent Palladium-Catalyzed Cyclization

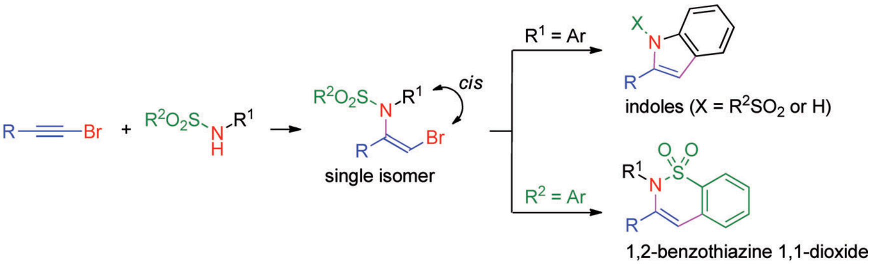

Bromine as a double agent: The bromine atom in 1-bromo-1-alkynes works as an electron-withdrawing group to effect the nucleophilic addition of sulfonamides. It again plays a pivotal role in the palladium-catalyzed cyclization of the resultant (*Z*)-2-(sulfonylamino)-1-bromoalkenes into nitrogen heterocycles (see scheme).

PEG-DNAzymes

H. Abe,* N. Abe, A. Shibata, K. Ito, Y. Tanaka, M. Ito, H. Saneyoshi, S. Shuto, Y. Ito* ________ **6475 – 6479**

Structure Formation and Catalytic Activity of DNA Dissolved in Organic Solvents

Equal-opportunity dissolver: By attaching polyethylene glycol at its 5′ end, DNA (PEG-DNA) can be solubilized in various organic solvents and was shown to form G-quadruplexes by CD spectroscopy. A complex containing iron(III) protoporphyrin IX (hemin) and G-quadruplex-forming PEG-DNA catalyzed an oxidative reaction in methanol (see scheme).

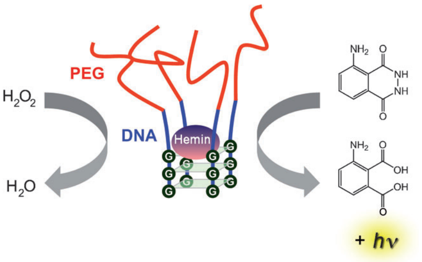

Asymmetric Catalysis

B. M. Trost,* K. Hirano ____ **6480 – 6483**

Highly Stereoselective Synthesis of α-Alkyl-α-Hydroxycarboxylic Acid Derivatives Catalyzed by a Dinuclear Zinc Complex

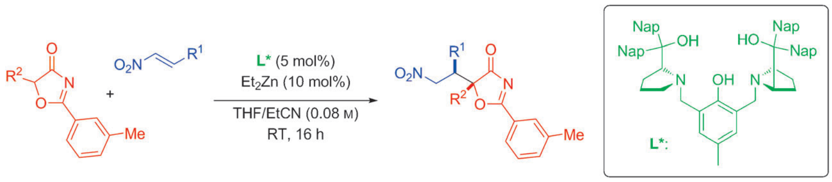

A dinuclear zinc–ProPhenol catalyst enables highly enantioselective nitro-Michael reactions with oxazol-4(5*H*)-ones as nucleophilic substrates (see scheme, Nap = 2-naphthyl). This work highlights the utility of the ProPhenol family of ligands. The modular nature of these ligands proved crucial in the optimization of reaction conditions to achieve excellent stereoselectivities.

Natural Product Synthesis

Z.-Y. Yang, H.-Z. Liao, K. Sheng, Y.-F. Chen, Z.-J. Yao* ______ **6484 – 6487**

Enantioselective Total Synthesis of Marine Diterpenoid Clavulactone

The key steps in the synthesis of clavulactone are formation of an enantiopure cyclopentane precursor by epoxide rearrangement and intramolecular carbonyl–ene reaction, construction of the 3,4-dihydro-2*H*-pyran ring by intermolecular hetero-Diels–Alder reaction, closure of the eleven-membered ring, and finally generation of the lactone functionality by chemoselective allylic C(sp^3)—H oxidation.

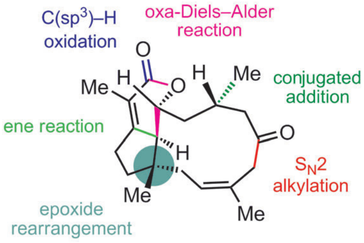

clavulactone

C–H Functionalization

R. T. Gephart III, D. L. Huang,
M. J. B. Aguila, G. Schmidt, A. Shahu,
T. H. Warren* ______ 6488 – 6492

Catalytic C–H Amination with Aromatic Amines

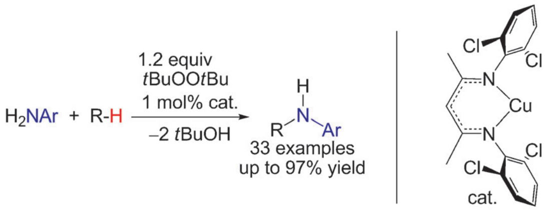

Aniline joins the club: A β-diketiminato copper(I) catalyst enables C–H amination of anilines employing low catalyst loadings to preclude oxidation to the diazene ArN=NAr (see scheme). Electron-poor anilines are particularly resistant towards diazene formation and participate in the amination of strong and unactivated C–H bonds. N-alkyl anilines also take part in C–H amination.

Synthetic Methods

Y.-F. Chen, M. Chen,
Y.-H. Liu* ______ 6493 – 6497

Gold-Catalyzed Cascade Cyclizations of 1,6-Diynyl Carbonates to Benzo[*b*]fluorenes Involving Arylation of Oxocarbenium Ion Intermediates and Decarboxylative Etherification

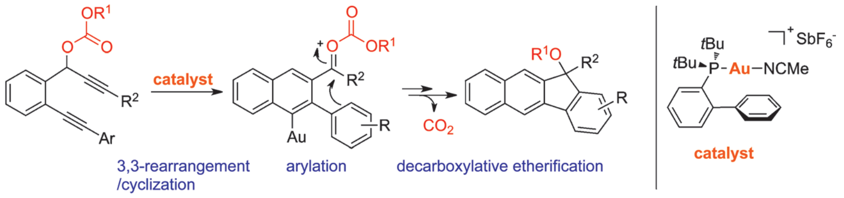

Rearranged: The described gold-catalyzed cycloisomerizations give access to highly substituted benzo[*b*]fluorenes under mild reaction conditions (see scheme). Experimental results indicate that the in situ formed oxocarbenium ion intermediates, derived from gold-catalyzed 3,3-rearrangement and 6-*endo-dig* cyclization, undergo intramolecular arylation and subsequent decarboxylative etherification to furnish the final ether products.

Thermal Transport Materials

W.-L. Song, P. Wang, L. Cao, A. Anderson,
M. J. Meziani, A. J. Farr,
Y.-P. Sun* ______ 6498 – 6501

Polymer/Boron Nitride Nanocomposite Materials for Superior Thermal Transport Performance

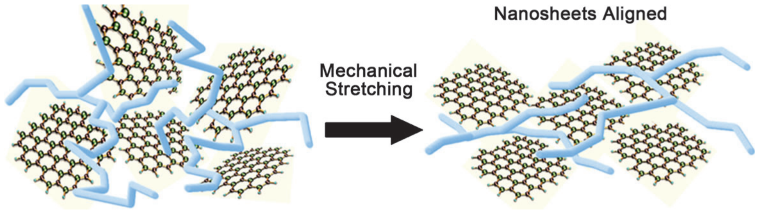

Boron nitride nanosheets were dispersed in polymers to give composite films with excellent thermal transport performances approaching the record values found in polymer/graphene nanocomposites. Similarly high performance at lower BN loadings was achieved by aligning the nanosheets in poly(vinyl alcohol) matrix by simple mechanical stretching (see picture).

Protein Modifications

M. Lo Conte, K. S. Carroll* _ 6502 – 6505

Chemoselective Ligation of Sulfinic Acids with Aryl-Nitroso Compounds

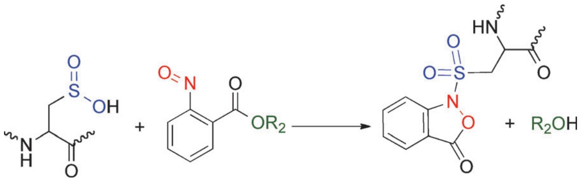

Making a comeback: The inefficient condensation of sulfinic acid and aryl nitroso compounds has been transformed into a chemoselective process that converts sulfinic acid into stable cyclic sulfonamide analogues (see scheme). This ligation proceeds rapidly under aqueous conditions in high yield, and lays the groundwork for the development of sulfinic acid detection methods in biological systems.

Doped nanocrystals of $NaYF_4$ and $NaGdF_4$ are currently studied as upconversion luminescence markers and magnetic resonance imaging contrast agents. An EPR investigation on the growth mechanism of $NaYF_4$:Gd and $NaGdF_4$ nanocrystals showed that these nanomaterials grow in the standard oleic acid-based reaction medium by a dissolution/recrystallization mechanism and not by the aggregation or oriented attachment of smaller particles.

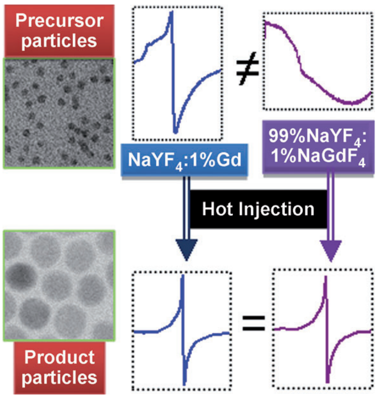

Nanocrystal Growth

R. Komban, J. P. Klare, B. Voss,
J. Nordmann, H.-J. Steinhoff,*
M. Haase* ______ **6506 – 6510**

An Electron Paramagnetic Resonance Spectroscopic Investigation on the Growth Mechanism of $NaYF_4$:Gd Nanocrystals

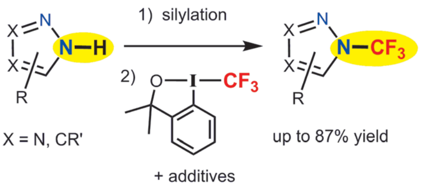

Effective CF_3 transfer: Various electron-rich nitrogen heterocycles (pyrazoles, triazoles, and tetrazoles) can be directly N-trifluoromethylated by a hypervalent iodine reagent in an efficient manner. The optimized procedure, which includes an in situ silylation of the substrate followed by an acid-catalyzed CF_3 transfer, provides ready access to a series of new and previously challenging or inaccessible NCF_3 compounds.

Direct N-Trifluoromethylation

K. Niedermann, N. Früh, R. Senn,
B. Czarniecki, R. Verel,
A. Togni* ______ **6511 – 6515**

Direct Electrophilic N-Trifluoromethylation of Azoles by a Hypervalent Iodine Reagent

Eraserhead: Stem cells seem to erase epigenetic information by decarboxylation of the newly discovered epigenetic base 5-carboxycytosine (caC; see picture). This reaction is likely to involve a nucleophilic attack of the C5–C6 double bond.

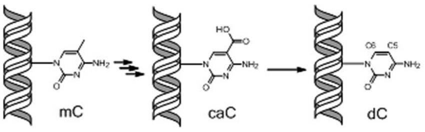

Epigenetics

S. Schiesser, B. Hackner, T. Pfaffeneder,
M. Müller, C. Hagemeier, M. Truss,*
T. Carell* ______ **6516 – 6520**

Mechanism and Stem-Cell Activity of 5-Carboxycytosine Decarboxylation Determined by Isotope Tracing

Rigid threads: Lacewings protect their eggs from predators by laying them on small stalks (see picture). The stalks have good mechanical properties and, unlike most other silks, a cross β structure. An artificial egg stalk was produced using a designed recombinant variant of a sequenced lacewing egg stalk protein, and it attained 90% of the tensile strength of a natural egg stalk.

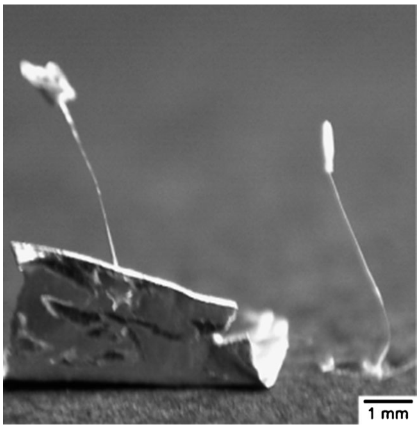

Biomaterials

F. Bauer, T. Scheibel* ______ **6521 – 6524**

Artificial Egg Stalks Made of a Recombinantly Produced Lacewing Silk Protein

Natural Product Synthesis

D. Hager, P. Mayer, C. Paulitz, J. Tiebes,
D. Trauner* ______ 6525 – 6528

Stereoselective Total Syntheses of Herbicidin C and Aureonuclemycin through Late-Stage Glycosylation

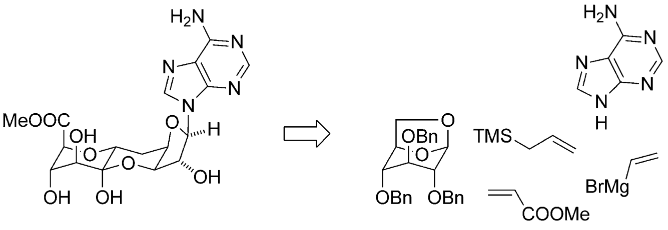

Better late than never! Two herbicidins, members of an important family of nucleoside antibiotics, have been synthesized for the first time. The route integrates a stereoselective C-glycosylation with several reagent-controlled stereoselective transformations and a surprisingly facile and highly diastereoselective late-stage N-glycosylation.

Cationic Phosphorus

T. Köchner, T. A. Engesser, H. Scherer,
D. A. Plattner, A. Steffani,
I. Krossing* ______ 6529 – 6531

$[P_9]^+[Al(OR^F)_4]^-$, the Salt of a Homopolyatomic Phosphorus Cation

Inside Cover

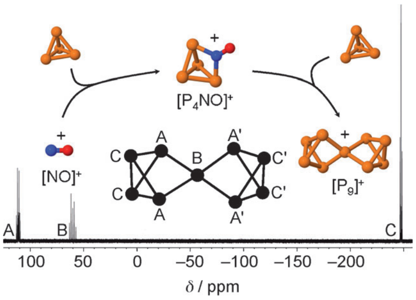

Positive at last: The first condensed-phase homopolyatomic phosphorus cation $[P_9]^+$ was prepared using a combination of the oxidant $[NO]^+$ and weakly coordinating anion, $[Al\{OC(CF_3)_3\}_4]^-$. $[P_9]^+$ consists of two P_5 cages linked by a phosphonium atom to give a D_{2d}-symmetric Zintl cluster. NMR (see picture), Raman, and IR spectroscopy, mass spectrometry, and quantum-chemical calculations confirmed the structure.

Supporting information is available on www.angewandte.org (see article for access details).

A video clip is available as Supporting Information on www.angewandte.org (see article for access details).

This article is available online free of charge (Open Access).

This article is accompanied by a cover picture (front or back cover, and inside or outside).

Service

Spotlight on Angewandte's Sister Journals ______ *6304 – 6306*

Preview ______ *6534*